(Received 11 September 2023, Accepted 13 December2023, Scheduled 20 December2023)

A Low RCS Design under a Large Incident Angle for the Curved Surface Edge Considering Edge Effects

Guanya Li*

National Engineering Research Center of Electromagnetic Radiation Control Materials
State Key Laboratory of Electronic Thin Film and Integrated Devices
University of Electronic Science and Technology of China, Chengdu, China

ABSTRACT: In the context of the backscatter problem caused by edge diffraction on metallic curved surface, this study proposes a method to mitigate the scattering effect by loading different metasurface structures in four equally divided regions along the surface edge. Based on the design of the loaded metasurface on the curved surface, the interaction between the reflection field on the surface and the diffracted field is regulated by adjusting two key parameters: the reference phase (φ_0) at the edge and the phase difference (φ_d) in adjacent regions. By controlling these parameters, reduction in the monostatic radar cross-section (RCS) can be achieved when the metasurface is loaded onto the curved surface. By controlling the reflection phase of a sandwich-like unit structure subjected to oblique incidence of electromagnetic waves, a metasurface that meets the requirements has been designed. Through a comparison and analysis of the near field and monostatic radar cross-section before and after loading the metasurface, the effectiveness of this design method is confirmed. This method is of great significance to control the electromagnetic scattering caused by edge diffraction.

1. INTRODUCTION

Under the illumination of radar wave, when strong scattering sources (such as specular surface [1, 2], cavity [3, 4], and dihedral corner [5, 6]) on detected targets are effectively controlled, and more attention should be paid to electromagnetic scattering from surface defects. Among them, the electromagnetic scattering caused by edge is an outstanding problem compared to other defect types which can be repaired by filling and coating material in a small area [7, 8]. Therefore, for low Radar Cross-Section (RCS) applications such as stealth technology, antenna, and RCS measurements, the suppression of edge scattering is crucial. It can be usually controlled by the combination of material property and geometry. Firstly, various different geometric shapes for the purpose of minimizing backscattering have been introduced [9–12]. Secondly, from the perspective of material property design, methods to suppress edge scattering include the use of edge-groove structures [13, 14] and edge coatings [15], among others, which have received significant attention. Edge scattering is an important phenomenon that can be explained as the scattering caused by the discontinuity impedance between the edge of the target object and its surrounding environment. So it is also useful to have gradient impedance loaded on edge [16–19]. Additionally, other related research includes the use of inhomogeneous anisotropic impedance surface to guide surface waves and suppress scattering from the oblique sides of triangular scatterers [20], as well as the utilization of soft and hard anisotropic impedance surfaces for redirecting backscattering [21, 22]. Edge scattering can also be controlled through encoding metasurface units [23, 24].

As mentioned above, edge loading technology is an important approach to address the issue of edge scattering in the low RCS design. This technique involves loading metamaterial or metasurface in the vicinity of the edge or on the edge surface to control the electromagnetic scattering caused by the edge. Common methods for mitigating edge scattering include the loading of gradient impedance surface, anisotropic impedance surface, soft-hard surface, and coding metasurface. These techniques are commonly used for the treatment of two-dimensional surface edge. In addition, it should be noted that edge diffraction is also an important physical mechanism affecting edge electromagnetic scattering, but the above design method does not fully analyze the influence of the design on the diffraction field, and existing works rarely design surface according to the characteristics of the edge diffraction field. In this paper, a metasurface design is proposed to tackle a three-dimensional curved surface edge based on the characteristics of edge diffraction fields and to suppress the edge scattering of curved surface. By calculating the magnitude and phase distribution of the edge diffraction field, the reflection phase distribution on the surface of the curved edge is controlled to reduce the backscattering when the edge is illuminated. And its influence on the edge diffraction field is analyzed.

When electromagnetic waves impinge on the metal edge, nonuniform diffracted fields are excited in the vicinity of the edge due to the presence of edge effects. Therefore, by studying the phase distribution of the electric field in the vicinity of the edge, a metasurface loading scheme based on the scattering cancellation principle is designed to suppress the backscattered energy. For simplification purposes, the incident angle of the plane wave is set to 90 degrees. To verify the backscattering suppression performance of this scheme, a series of simulations

* Corresponding author: Guanya Li (lgynhy@163.com).

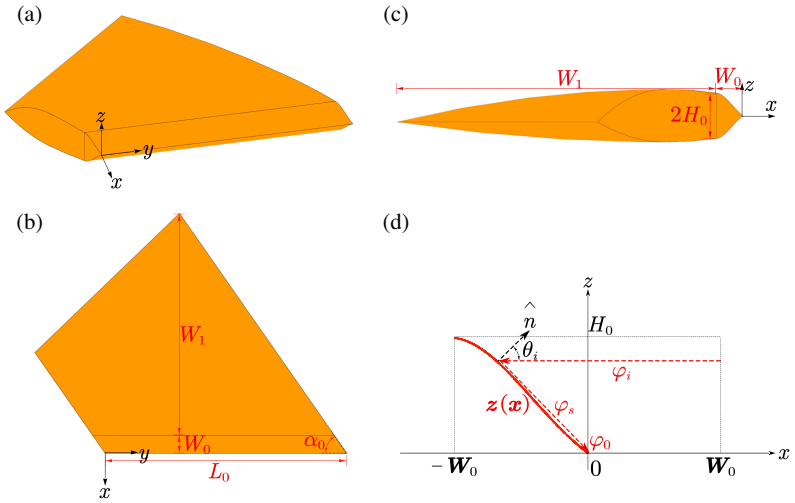

FIGURE 1. (a) 3D view of metal edge object; (b) Top view; (c) Side view; (d) Projected profile of the curved face on the *xoz* plane, and definition of φ_i and φ_s.

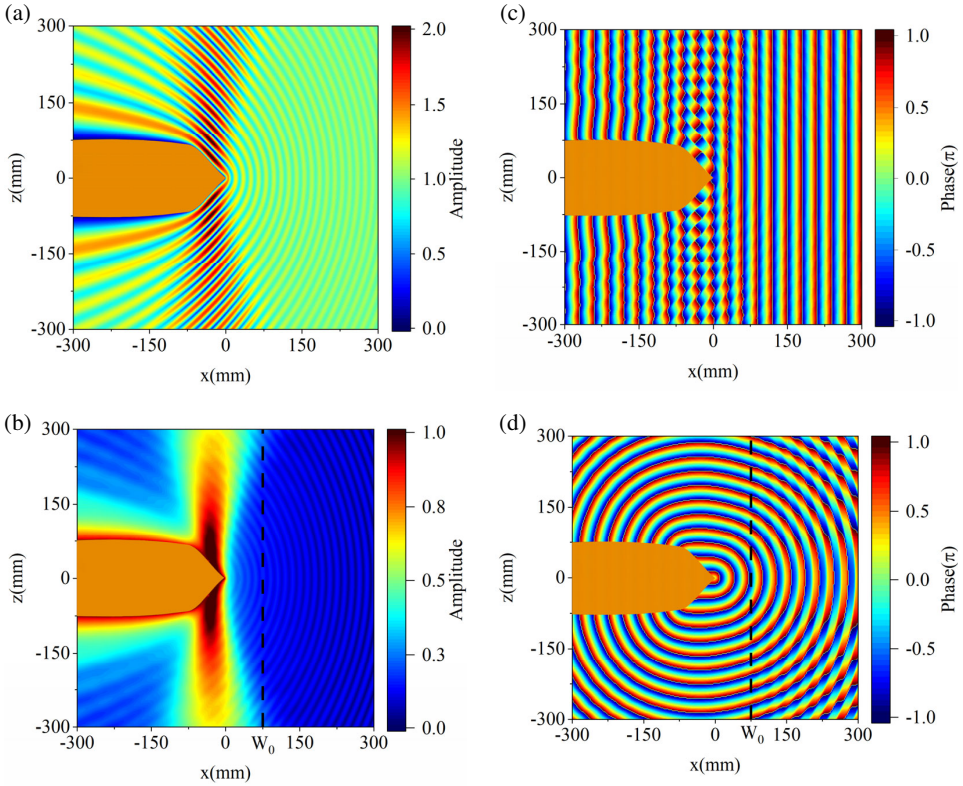

FIGURE 2. (a) Amplitude distribution of the total field; (b) Amplitude distribution of the reflection and diffracted field; (c) Phase of the total field; (d) Phase of the reflection and diffracted field.

are conducted. As expected, results demonstrate the effectiveness of this method in reducing the peak RCS caused by the edge. This method is valuable for low RCS applications especially for stealth technology.

2. ANALYSIS AND DESIGN

For the convenience of research and analysis, we consider the metallic edge structure shown in Figure 1(a) as the subject of our investigation. Figures 1(b) and (c) depict the top view and left view, respectively. The length L_0 is 1000 mm, and the width W_0 is 75 mm. The angle α_0 between the edge and the surface of right side is 55 degrees, and half of the edge thickness H_0 is 65 mm. Additionally, we have $W_1 = 915$ mm. Figure 1(d) illustrates the projection of the front edge contour line on the *xoz* plane, which satisfies an exponential equation:

$$z(x) = 24.45\left\{e^{1.40-[0.0158(x+W_0)]^2} - 1\right\} \quad (1)$$

When electromagnetic waves impinge on the edge structure, the electromagnetic field near the edge can be considered as the superposition of the incident field, the reflected field of the electromagnetic wave on the edge surface, and the diffracted field caused by the edge. When the electromagnetic wave is incident along the $-x$-axis direction and the E-field vector parallel to the edge, the amplitude and phase distribution of the total field near the edge are shown in Figures 2(a) and (c). By removing the plane wave incident illuminating from the right side, the superposition of the reflected field from the curved surface and the diffracted field caused by the edge are obtained. The amplitude and phase of this field are represented by Figures 2(b) and (d). Although the amplitude of the electric field on the upper and lower surface of the edge is large, it can be inferred from the normal direction of the equiphase surface near the curved surface that it contributes little to the backscattering. On the contrary, the diffracted field on the right side of the edge is the main source of backscattering, even though its amplitude is relatively small compared to the reflected field. When the reference plane is taken as the plane $x = W_0$, the amplitude and phase of the scattering field on this reference plane vary along the z-direction, as shown in Figure 3.

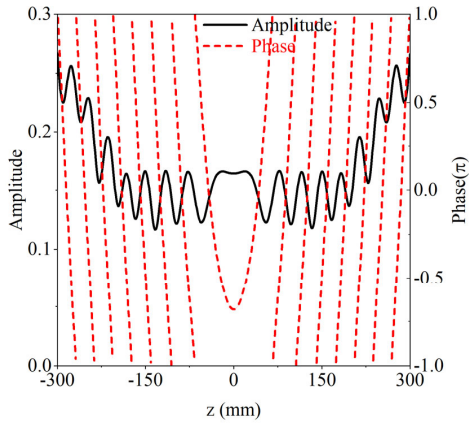

FIGURE 3. The amplitude and phase of the scattering field on plane $x = W_0$.

To enhance the interaction between the reflected field on the curved surface and the diffracted field, it can be tried to make the wavefront shape of the reflection field, and that of the diffraction field has similar characteristics. Since the diffracted field has a focal on the edge, it is possible to design an appropriate distribution of reflection phase on the surface that focuses the reflected field at the edge. Specifically, when a plane wave incident along the $-x$-axis direction reflects off the surface and reaches the edge, it should have the same phase φ_0. Therefore, the reflected phase distribution on the curved surface at the edge should satisfy the following condition:

$$\varphi_r = \varphi_0 - \varphi_s - \varphi_i \tag{2}$$

Here, φ_s refers to the wave phase difference from a point on the surface to the edge position, and φ_i represents the phase difference from the reference plane to a point on the curved surface (as shown in Figure 1(d)). When the reference plane is chosen as $x = W_0$, the above equation can be expressed as:

$$\varphi_r(\vec{r}_0) = \varphi_0 - k\left(\sqrt{x_0^2 + z_0^2}\right) + k(W_0 - x_0) \tag{3}$$

where $\vec{r}_0 = (x_0, y_0, z_0)$, and it represents the position vector of any point on the edge surface. k is the wave number of the incident wave. Because the amplitude of the reflected field is greater than that of the diffracted field, it is further considered to divide the curved surface into multiple regions, where the phase difference between the reflected fields of each adjacent region is φ_d ($\varphi_d \neq 0$), in order to reduce the amplitude of the total field in the x-direction across multiple regions. When dividing each surface into two parts equally along the y-axis direction, the reflection phase distribution in the j-th region satisfies:

$$\begin{aligned}\varphi_{rj}(x_0, y_0, z_0) \;=\; & \varphi_0 - k\left(\sqrt{x_0^2 + z_0^2}\right) + kx_0 \\ & + \varphi_d \, mod(j-1, 2)\end{aligned} \tag{4}$$

where *mod*$(j-1, 2)$ represents remainder of $j-1$ divided by 2. According to array theory [25], the total backscattered field can be expressed as:

$$E = \sum_{j=1}^{4} \sum_{m=1}^{n_y} \sum_{n=1}^{n_x} \left\{ \begin{array}{l} e^{-i[2\varphi_i(\vec{r}_{0mn}) + \varphi_{rj}(\vec{r}_{0mn})]} \\ + A_{W_0}(z_{0mn}) e^{-i\varphi_{W_0}(z_{0mn})} \end{array} \right\} \tag{5}$$

where $\vec{r}_{0mn}$ represents the center point of unit in the m-th row and n-th column on the surface; n_x and n_y represent the number of units in the x-direction and y-direction for the j-th region, respectively. A_{W_0} and φ_{W_0} represent the amplitude and phase on the reference plane $x = W_0$ (as shown in Figure 3).

Figure 4(a) illustrates the influence of the variations in φ_0 and φ_d on the normalized amplitude of the total backscattered field. It can be observed that the amplitude of the total field reaches its minimum when $\varphi_0 = 1.56\pi$ and $\varphi_d = 0.59\pi$. At this point, the reflection phase distribution on the curved surface corresponds to Figure 4(b).

3. DESIGN OF STRUCTURE

To perfectly realize the metasurface discussed in the aforementioned section, the structure shown in Figures 5(a) and (b) is selected as the basic unit cell to achieve the predetermined reflection phase. This unit is a typical sandwich structure with a full metal bottom layer, a middle dielectric layer with permittivity of 2.2 and thickness of $t = 3$ mm, and a top layer of octagonal metal patterns. The pattern is with a period of $p = 8$ mm, and its two other key dimensional parameters are angle α and periodic spacing g, where α ranges from 0.5π to 1.5π. The size of this angle determines whether the top metal pattern is more square (when α is close to 0.5π) or star-shaped (when α is close to 1.5π). When the electromagnetic wave is normally incident on this unit, by changing the shape of the top pattern through the above two parameters, different reflection phases as illustrated in Figure 5(c) can be obtained by the frequency domain solver of CST software under unit-cell boundary. In order to make the range of reflection phase close to 2π and make the phase

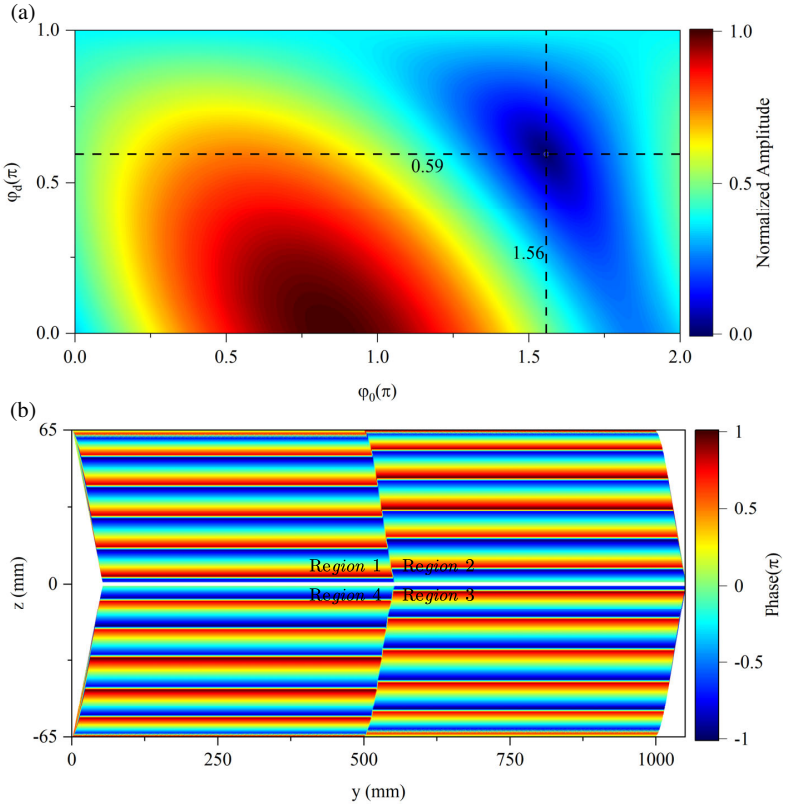

FIGURE 4. (a) Normalized amplitude of the total backscattered field; (b) Reflection phase distribution on curved surface.

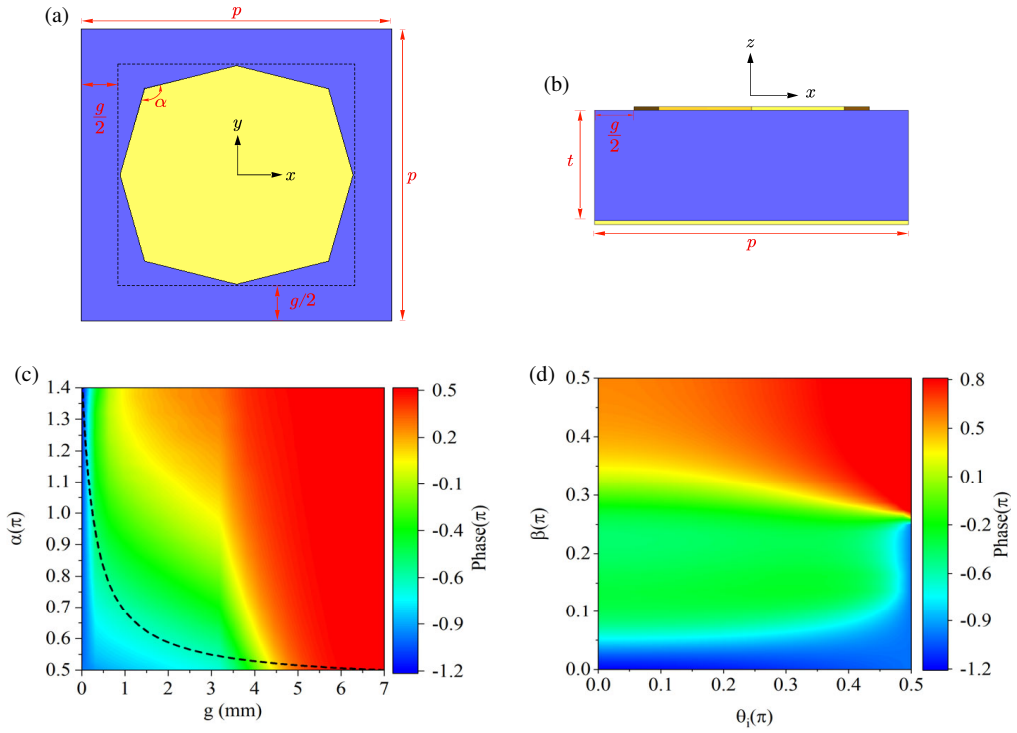

FIGURE 5. (a) Top view of the unit cell; (b) Side view; (c) The reflection phase of unit structures with different structural parameters g and α when electromagnetic waves are incident perpendicular to the surface at 10 GHz; (d) The reflection phase of different structure defined by β in different incident angle at 10 GHz.

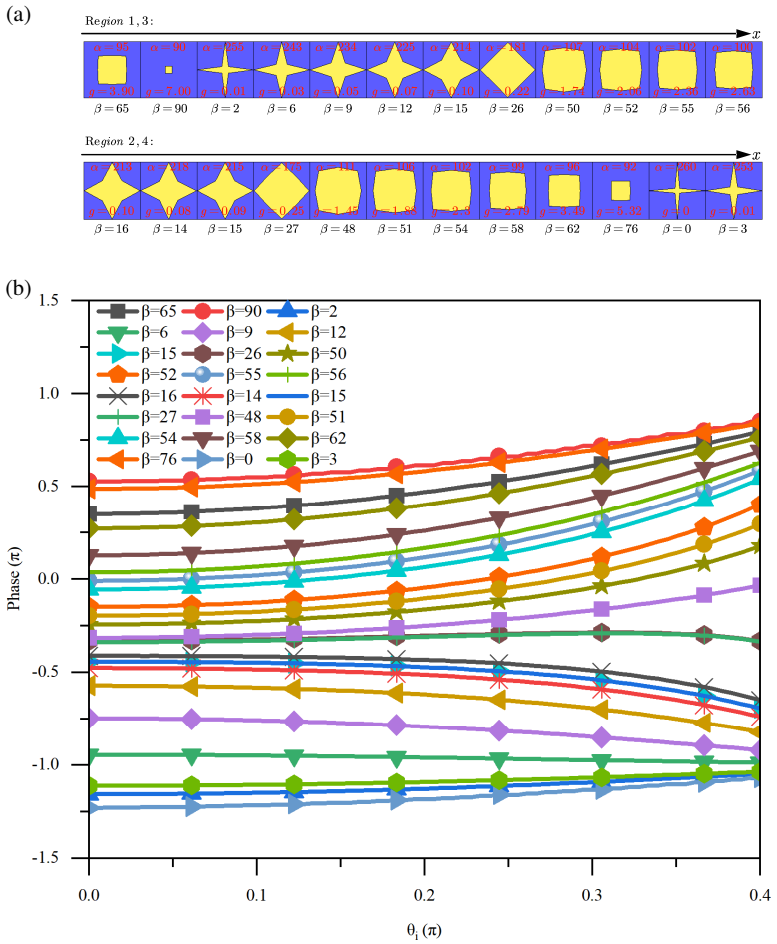

FIGURE 6. (a) Units for the design results and the values of parameter g and α; (b) The variation of reflection phase with the angle of incidence for different units at 10 GHz.

change more smoothly with the size parameter, the structural parameters can be selected along path C in Figure 5(c). For convenience, the parameter equations as the two variables α and g vary along this path are given as:

$$g = 3.3 + \frac{3.5\sqrt{[\tan(0.017\beta) - 0.957]^2 + 0.171} - 3.6}{\tan(0.017\beta)} \quad (6)$$

$$\alpha = 0.47\sqrt{[\tan(0.017\beta) - 0.957]^2 + 0.171} - 0.49\tan(0.017\beta) + 0.95 \quad (7)$$

That is, when parameter β is determined, g and α values of the basic unit can be obtained. In other words, each β corresponds to a certain top metal pattern. β can range from 0 to 0.5π. For the curved surface, when the incident angle of the electromagnetic wave is specified, for the unit structures at different positions on the surface, the angle between the incident direction of the electromagnetic wave and the normal direction of the surface at that point is different, that is, the actual incident angle is different. Therefore, it is also necessary to examine the variation of the reflection phase of the above unit structure under different oblique incident angles. When the incident direction of the electromagnetic wave is along $-x$-axis, the actual incident angle (the angle between the incident direction and the normal direction of the incident point on surface as shown in Figure 1(d)) at each point on the surface satisfies the relationship:

$$\theta_i = \text{atan}\left[\frac{1}{-z'(x_0)}\right] \quad (8)$$

x_0 is the x coordinate of a point on the surface. This means that each unit on the surface has an actual angle of incidence that varies with x_0. As shown in Figure 5(d), when the incident angle and desired reflection phase are given, a top pattern can be uniquely determined from that. The parameter β that meets the requirement can be selected to determine its dimensional parameters α and g according to Figure 5(d).

The shapes of units used in the final design are shown in Figure 6(a). The parameters α and g of the top pattern of each unit are indicated in the figure. Note that α in the figure corresponds to the unit of degree, and g corresponds to the unit of mm. The parameter β of each unit for equations (6)∼(7) is also given. In this design, the incident angle of electromagnetic wave along $-x$ direction is considered. At this time, the incident angle of each point on the curved surface can be calculated from formula (8), and the variation range is $0.23\pi \sim 0.4\pi$. The reflection phase variation of the units shown in Figure 6(a) at different

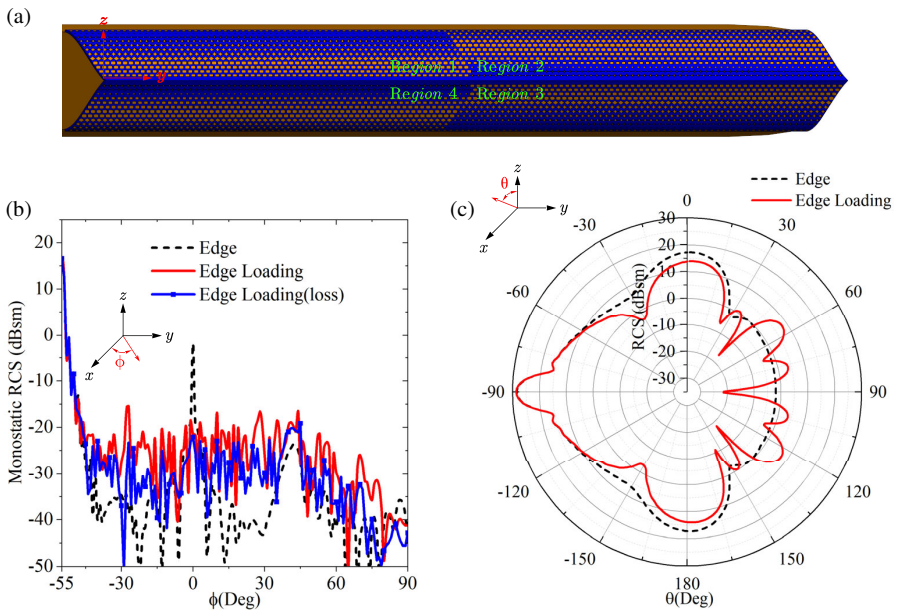

FIGURE 7. (a) Edge loaded with the purposed metasurface; (b) Monostatic RCS for electromagnetic waves incident from different azimuth angles when electric field is perpendicular to z axis; (c) The bistatic RCS for electromagnetic wave incident along the $-x$ axis direction with E-field parallel to the edge.

incident angles with an incident wave frequency of 10 GHz can be expressed as Figure 6(b). It can be seen that the reflection phase of the selected units could shift to a certain extent when the incident angle changes, but the phase shift range of most of the selected units is not large, and the shift amplitude is within the acceptable range.

4. SIMULATION AND VERIFICATION

The phase distribution on the surface specified by Figure 4(b) can be achieved by obtaining the structural parameters that correspond to the desired reflection phase at each position on the surface according to Figure 5(d). The surface edge loaded with the metasurface that realizes this reflection phase distribution is depicted in Figure 7(a). To validate the effectiveness of the proposed surface structure, electromagnetic scattering analysis of the surface edge loaded with the aforementioned structure was performed using Feko software and MLFMM technique at 10 GHz.

As shown in Figure 7(b), the monostatic RCS of the edge loaded with metasurface is reduced by 19.5 dB at the azimuth $\phi = 0$, and the average RCS is -27.6 dB in the range of $-50 \sim 90$ degrees. When electromagnetic waves are incident along the $-x$-axis direction, from the bistatic RCS depicted in Figure 7(c), it can be seen that the scattering pattern is divided into upper and lower parts. The proposed design successfully eliminates the peak scattering in the x-axis direction, achieving the intended design goals. However, it also leads to an increase in monostatic RCS at certain azimuth angles. To address this issue, further analysis was conducted as follows. Firstly, the proposed loading scheme utilizes lossless dielectric plates, redistributing the energy scattered by the edge in the spatial angular domain without energy loss compared to the case before loading. Therefore, it is possible to consider increasing the dielectric loss to reduce the monostatic RCS at azimuth angles other than the peak value. The blue curve in Figure 7(b) represents the monostatic RCS with a dielectric loss tangent of 0.05. Compared to the case with lossless dielectric plates, the monostatic RCS at non-peak azimuth angles is somewhat controlled. Secondly, the design assumes the incident direction of the electromagnetic wave along the $-x$ direction, which also leads to the aforementioned issue. In future work, further optimization design can be considered for a certain angular domain. Additionally, in practical engineering applications, after certain treatments on the edge, absorbing materials are often loaded on the edge to further control electromagnetic scattering.

The near-field distribution of the proposed structure is as shown in Figure 9. Compared with Figures 2(b) and (d), it can be seen that the scattering on the curved surface loaded with metasurface has multiple maximum value regions. Additionally, from Figure 9(c), it can be seen that the magnitude and phase of the scattering field are asymmetric on the $x = W_0$ plane (that of the original metal edge is symmetric about $z = 0$ on this plane as shown in Figure 3). Moreover, as can be seen from Figure 9(d), the real part of the electric field in the region near the edge approximately satisfies the anti-symmetric relationship. This phenomenon is manifested as RCS reduction in a specific direction in the far field. In general, the metasurface on curved surface based on the characteristics of edge diffraction field can adjust the edge scattering field and suppress the backscattering intensity of the edge when the electromagnetic wave is incident at a large angle.

When the electromagnetic wave incident direction is fixed at different elevation angles, the curve of the monostatic RCS variation with azimuth angle is shown in Figure 8(a). When the incident direction elevation angle is 90 degrees, the electromag-

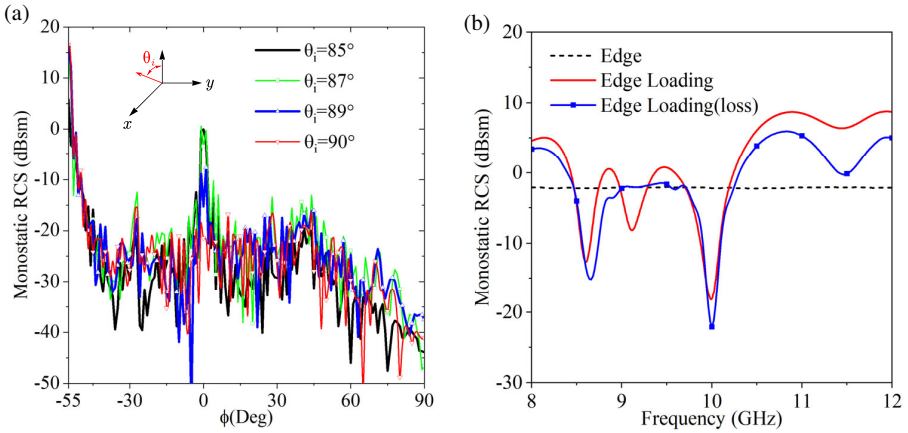

FIGURE 8. (a) Curve of the monostatic RCS variation with azimuth angle for the edge with loading when the electromagnetic wave incident direction is fixed at different elevation angles; (b) The variation of monostatic RCS with frequency.

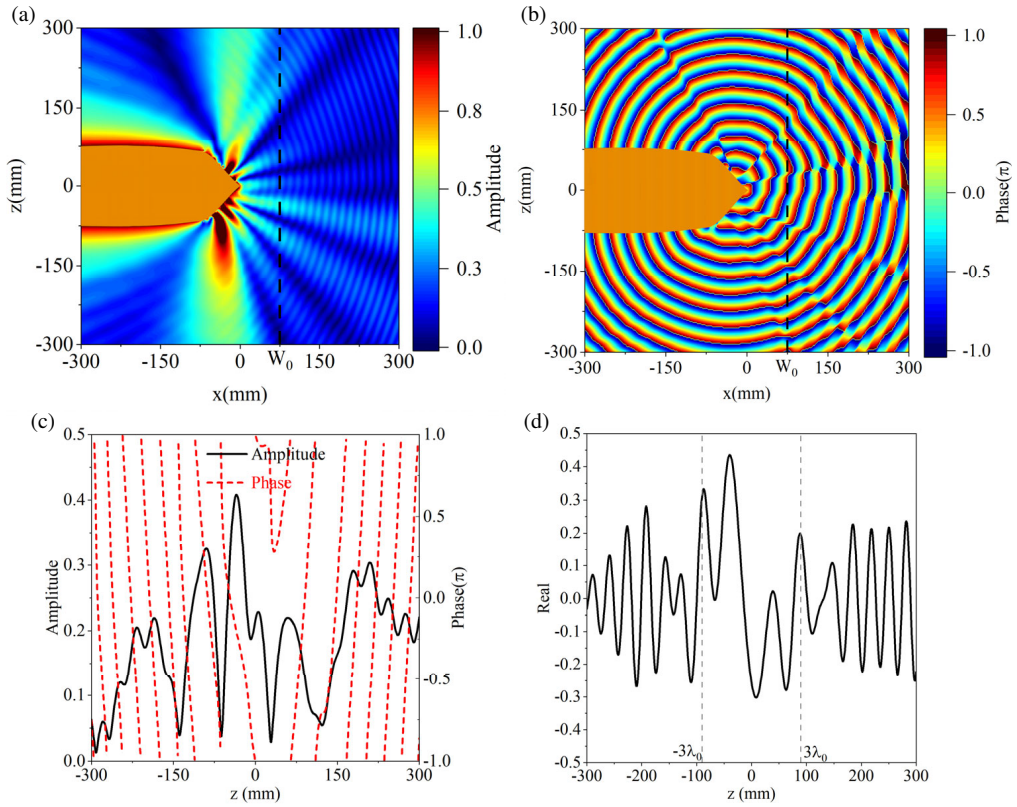

FIGURE 9. Amplitude and phase of the reflection and scattering field for the edge loaded with purposed metasurface; (a) Amplitude distribution of the reflection and scattering field; (b) Phase distribution of reflection and scattering field; (c) The amplitude and phase of the scattering field on plane $x = W_0$; (d) The real part of the scattering field on plane $x = W_0$.

netic wave is incident along the $-x$ axis direction. It can be seen that the monostatic RCS near the azimuth angle of 0 degrees is sensitive to the changes in elevation angle. Around the azimuth angle of 0 degrees, when the incident wave deviates from the $-x$ axis direction, the monostatic RCS increases. However, an interesting phenomenon to note is that there is always a local minimum point of the monostatic RCS at the azimuth angle of 0 degrees within a certain range of elevation angles. The above variations are closely related to the electromagnetic wave incident conditions considered in the structural design. In further design, to overcome the sensitivity of the monostatic RCS to changes in elevation angle, the differences in diffraction fields of electromagnetic waves from different incident directions on the edge need to be considered.

The variation of monostatic RCS with frequency is shown in Figure 8(b). The blue curve with square markers represents the RCS of the structure designed with a substrate of dielectric loss tangent of 0.05. The red curve corresponds to the case that the

dielectric loss of the substrate is 0. It can be observed that the designed structure exhibits a significant reduction in edge RCS at 10 GHz. The introduction of loss in the design not only further decreases the monostatic RCS at 10 GHz but also controls the RCS at two deteriorating frequencies, 8.8 GHz and 9.5 GHz, on the red curve. Overall, this design effectively reduces the monostatic RCS at the target frequency, but the reduction bandwidth is limited. Further design and optimization are expected in future work to achieve a wider reduction bandwidth.

5. CONCLUSION

In the design of structures with low RCS at edge of curved surface, the interaction between reflected and diffracted fields can be enhanced by appropriate reflection phase distribution based on the principle of reflection and diffraction. When the curved surface is divided into a plurality of regions, the amplitude of the total field in the x-axis direction is reduced by adjusting the phase difference (φ_d) of the reflected field of each pair of adjacent regions, so that backward electromagnetic scattering is suppressed when the electromagnetic wave is incident at a large angle. The design method is effective to reduce the backscattering of the curved surface edge structure. This method is of great significance to control the electromagnetic scattering caused by edge diffraction. And it provides an alternative design approach for suppressing edge scattering without altering the physical geometry, offering advantages such as ease of manufacturing, light weight, and thin thickness. It has certain application value in aircraft edge scattering control as well.

REFERENCES

[1] Yang, X. M., G. L. Jiang, X. G. Liu, and C. X. Weng, "Suppression of specular reflections by metasurface with engineered nonuniform distribution of reflection phase," *International Journal of Antennas and Propagation*, Vol. 2015, 1–8, 2015.

[2] Zhou, Y., G. Zhang, H. Chen, P. Zhou, X. Wang, L. Zhang, L. Zhang, J. Xie, and L. Deng, "Design of phase gradient coding metasurfaces for broadband wave modulating," *Scientific Reports*, Vol. 8, 8672, Jun. 2018.

[3] Zhou, Y., Y. Yang, J. Xie, H. Chen, G. Zhang, F. Li, L. Zhang, X. Wang, X. Weng, P. Zhou, X. Li, and L. Deng, "Broadband RCS reduction for electrically-large open-ended cavity using random coding metasurfaces," *Journal of Physics D: Applied Physics*, Vol. 52, 315303, Jul. 2019.

[4] Chou, R.-C., "Reduction of the radar cross section of arbitrarily shaped cavity structures," Ph.D. dissertation, University of Illinois, 1987.

[5] Yin, H. and P. Huang, "PO analysis for RCS of nonorthogonal dihedral corner reflectors coated by RAM," *Journal of Systems Engineering and Electronics*, Vol. 12, No. 4, 1–6, 2001.

[6] Knott, E. F., "RCS reduction of dihedral corners," *IEEE Transactions on Antennas and Propagation*, Vol. 25, No. 3, 406–409, 1977.

[7] Sang, J., Z. Zhang, and S. Wang, "Research on the radar cross section of weak scatterers on stealth vehicle," *Advances in Aeronautical Science and Engineering*, Vol. 3, 257–262, 2012.

[8] Chen, H., J. Xie, P. Zhou, H. Lu, and L. Deng, "Research progress of repairing materials of electromagnetic discontinuities," *Materials China*, Vol. 32, 487–491, 2013.

[9] Ufimtsev, P. Y., "Method of edge waves in the physical theory of diffraction," *U.S. Air Force Foreign Technology Division Wright Pattern AFB*, Ohio, 1971.

[10] Jenn, D. C., *Radar and Laser Cross Section Engineering*, American Institute of Aeronautics and Astronautics Inc., Reston, Virginia, 2019.

[11] Liu, D., J. Huang, L. Song, and J. Ji, "Influence of aircraft surface distribution on electromagnetic scattering characteristics," *Chinese Journal of Aeronautics*, Vol. 30, No. 2, 759–765, Apr. 2017.

[12] Hassan, T. and M. Adnan, "Radar cross section based shape optimization of chine forebody," in *2022 19th International Bhurban Conference on Applied Sciences and Technology (IBCAST)*, 999–1004, 2022.

[13] Lee, W.-S., S.-J. Lee, D.-J. Lee, W.-S. Lee, and J.-W. Yu, "Scattering from concave conducting wedges with longitudinal corrugations: TM case," *Journal of Electromagnetic Waves and Applications*, Vol. 26, No. 16, 2142–2153, 2012.

[14] Lee, W.-S., S.-J. Lee, D.-J. Lee, W.-S. Lee, and J.-W. Yu, "TE scattering from concaved wedges with longitudinal corrugations," *IEEE Transactions on Antennas and Propagation*, Vol. 61, No. 4, 2355–2359, Apr. 2013.

[15] Smith, F. C., "Edge coatings that reduce monostatic RCS," *IEE Proceedings - Radar, Sonar and Navigation*, Vol. 149, No. 6, 310–314, Dec. 2002.

[16] Knott, E. F., "Suppression of edge scattering with impedance strings," *IEEE Transactions on Antennas and Propagation*, Vol. 45, No. 12, 1768–1773, Dec. 1997.

[17] Chen, H.-Y., L.-J. Deng, P.-H. Zhou, and J.-L. Xie, "Tapered impedance loading for suppression of edge scattering," *IET Microwaves Antennas & Propagation*, Vol. 5, No. 14, 1744–1749, Nov. 2011.

[18] Chen, H. Y., G. Y. Li, L. J. Lu, D. F. Liang, X. L. Weng, H. Y. Xie, and L. J. Deng, "Design of tapered periodic meta-surfaces for suppressing edge electromagnetic scattering," in *Materials Science Forum*, Vol. 998, 203–208, 2020.

[19] Zhu, Z.-W., H.-Y. Chen, H.-B. Zhang, P.-H. Zhou, L.-J. Deng, and J. Xie, "Patterned resistive strip loading for edge scattering suppression of a finite wedge," *Progress In Electromagnetics Research M*, Vol. 25, 27–38, 2012.

[20] Hou, H., J. Long, J. Wang, and D. F. Sievenpiper, "Reduced electromagnetic edge scattering using inhomogeneous anisotropic impedance surfaces," *IEEE Transactions on Antennas and Propagation*, Vol. 65, No. 3, 1193–1201, Mar. 2017.

[21] Quarfoth, R. and D. Sievenpiper, "Alteration of electromagnetic scattering using hard and soft anisotropic impedance surfaces," *IEEE Transactions on Antennas and Propagation*, Vol. 63, No. 10, 4593–4599, Oct. 2015.

[22] Li, G., Y. Liu, Q. He, H. Chen, X. Weng, D. Liang, J. Xie, and L. Deng, "Design of soft and hard composite patterns for electromagnetic scattering controlling at both normal and grazing incidence," *Microwave and Optical Technology Letters*, Vol. 64, No. 9, 1565–1571, Sep. 2022.

[23] Zhou, Y., X.-Y. Cao, J. Gao, S. Li, and X. Liu, "RCS reduction for grazing incidence based on coding metasurface," *Electronics Letters*, Vol. 53, No. 20, 1381–1382, Sep. 2017.

[24] Li, X., M. Feng, J. Wang, Y. Meng, J. Yang, T. Liu, R. Zhu, and S. Qu, "Suppressing edge back-scattering of electromagnetic waves using coding metasurface purfle," *Frontiers in Physics*, Vol. 8, Sep. 2020.

[25] Hansen, R. C., *Phased Array Antennas*, John Wiley & Sons, Chichester, 2009.